

1 Mapping of West Siberian taiga wetland complexes using Landsat 2 imagery: Implications for methane emissions

3 Terentieva I. E.^{1*}, Glagolev M. V.^{1,2,3,4}, Lapshina E. D.², Sabrekov A. F.¹ and
4 Maksyutov S.⁵

5 [1] {Tomsk State University, Tomsk, Russia}

6 [2] {Yugra State University, Khanty-Mansyisk, Russia}

7 [3] {Moscow State University, Moscow, Russia}

8 [4] {Institute of Forest Science, Moscow region, Russia}

9 [5] {National Institute for Environmental Studies, Tsukuba, Japan}

10 [*] {previously published as Kleptsova I. E.}

11 Correspondence to: I. E. Terentieva (kleptsova@gmail.com)

12

13 Abstract

14 High latitude wetlands are important for understanding climate change risks because these
15 environments sink carbon dioxide and emit methane. Fine-scale heterogeneity of wetland
16 landscapes poses a serious challenge when generating regional-scale estimates of greenhouse
17 gas fluxes from point observations. To reduce uncertainties at the regional scale, we mapped
18 wetlands and water bodies in the taiga zone of The West Siberia Lowland (WSL) on a scene-
19 by-scene basis using a supervised classification of Landsat imagery. Training data consists of
20 high-resolution images and extensive field data collected at 28 test areas. The classification
21 scheme aims at supporting methane inventory applications and includes 7 wetland ecosystem
22 types comprising 9 wetland complexes distinguishable at the Landsat resolution. To merge
23 typologies, mean relative areas of wetland ecosystems within each wetland complex type were
24 estimated using high-resolution images. Accuracy assessment based on 1082 validation
25 polygons of 10×10 pixel size indicated an overall map accuracy of 79%. The total area of the
26 WS wetlands and water bodies was estimated to be 52.4 Mha or 4-12% of the global wetland
27 area. Ridge-hollow complexes prevail in WS's taiga zone accounting for 33% of the total
28 wetland area, followed by pine bogs or "ryams" (23%), ridge-hollow-lake complexes (16%),
29 open fens (8%), palsa complexes (7%), open bogs (5%), patterned fens (4%), and swamps (4%).

1 Various oligotrophic environments are dominant among wetland ecosystems, while poor fens
2 cover only 14% of the area. Because of the significant change in the wetland ecosystem
3 coverage in comparison to previous studies, a considerable reevaluation of the total CH₄
4 emissions from the entire region is expected. A new Landsat-based map of WS's taiga wetlands
5 provides a benchmark for validation of coarse-resolution global land cover products and
6 wetland datasets in high latitudes.

7

8 **1 Introduction**

9 High latitude wetlands are important for understanding climate change mechanism as they
10 provide long term storage of carbon and emit significant amount of methane. The West Siberia
11 Lowland (WSL) is the world's largest high-latitude wetland system and experiences an
12 accelerated rate of climate change (Solomon et al., 2007).

13 Poorly constrained estimates of wetland and lake area constitute a major uncertainty in
14 estimating current and future greenhouse gas emissions (Melton et al., 2013; Turetsky et al.,
15 2014; Petrescu et al., 2010). Although wetland extent in WSL has been reasonably well
16 captured by global products based on topographic maps (Lehner and Döll, 2004; Matthews and
17 Fung, 1987), fine-scale heterogeneity of WSL's wetland landscapes (Bohn et al., 2007) requires
18 adding fine scale information in ecosystem functioning as made in wetland CH₄ emission
19 inventory (Glagolev et al., 2011) and estimates of net primary production (Peregon et al., 2008).
20 Present land cover products fail to capture fine-scale spatial variability within WSL's wetlands
21 because of lack of detail necessary for reliable productivity and emissions estimates. Frey and
22 Smith (2007) mentioned insufficient accuracy of four global vegetation and wetland products
23 with the best agreement of only 56% with the high-resolution WSL Peatland Database
24 (WSLPD) (Sheng et al., 2004). Products derived primarily from coarse-resolution microwave
25 remote sensing data (Prigent et al., 2007; Jones et al., 2010; Papa et al., 2010; Schroeder et al.,
26 2010; Schroeder et al., 2015) generally map the presence of surface water in the landscape, thus
27 overlooking non-inundated, CH₄-emitting wetlands in which the water table is at or below the
28 soil/peat or sphagnum surface. Because boreal peatlands does not experience prolonged
29 inundation, such products underestimate their area (Krankina et al., 2008). Uncertainty in
30 wetland inventory results in severe biases in CH₄ emission estimates, the scale of differences
31 has been shown by Bohn et al. (2015).

1 Modelers simulating methane emission are in need for high-resolution wetland maps that do
2 not only delineate wetlands but also identify the major sub-types to which different
3 environmental parameters could potentially be applied (Bohn et al., 2015). Several wetland
4 maps have been used to define the wetland extent in WSL, however their application to net
5 primary production (NPP) and methane emission inventories was accompanied by difficulties
6 due to crude classification scheme, limited ground truth data and low spatial resolution. One
7 peatland typology map that distinguishes several vegetation and microtopography classes and
8 their mixtures was developed at the State Hydrological Institute (SHI) by Romanova et al.
9 (1977). Peregon et al. (2005) digitized and complemented this map by estimating the fractional
10 coverage of wetland structural components using Landsat images and aerial photographs for
11 five test sites. However, the limited amount of fractional coverage data and coarse resolution
12 still result in large uncertainties in upscaling methane fluxes (Kleptsova et al., 2012).

13 Our goal was to develop a multi-scale approach for mapping wetlands using Landsat imagery
14 with a resolution of 30 m so the results could better meet the needs of land process modelling
15 and other applications concerning methane emission from peatlands. In this study, the WSL
16 taiga zone was chosen as the primary target for the land cover classification due to wetland
17 abundance. The objectives were: first, to develop a consistent land cover of wetland classes and
18 its structural components; second, to provide the foundation for environmental parameter
19 upscaling (greenhouse gas inventories, carbon balance, NPP, net ecosystem exchange, biomass,
20 etc) and validation of the process models.

21

22 **2 Materials and Methods**

23 **2.1 Study Region**

24 The West Siberian Lowland is a geographical region of Russia bordered by the Ural Mountains
25 in the west and the Yenisey River in the east; the region covers 275 Mha within 62-89°E and
26 53-73°N. Because of its vast expanse and flat terrain, the vegetation cover of the Lowland
27 shows clear latitudinal zonation. According to Gvozdetsky (1968), the taiga zone is divided into
28 three geobotanical subzones: northern taiga, middle taiga and southern taiga. Taiga corresponds
29 to the raised string bog province and covers about 160 Mha in the central part of the WS. It is
30 characterized by flat terrain with elevations of 80 to 100 m above sea level rising to about 190
31 m in the «Siberian Uvaly» area. Average annual precipitation is about 450-500 mm and

1 evaporation is 200-400 mm (National Atlas of Russia, 2008). The excess water supply and flat
2 terrain with poor drainage provides favorable conditions for wetland formation. Comprehensive
3 synthesis of Russian literature regarding the current state of the WSL peatlands, their
4 development and sensitivity to climatic changes was made by Kremenetski et al. (2003).

5 **2.2 Classification methodology**

6 No single classification algorithm can be considered as optimal methodology for improving
7 vegetation mapping; hence, the use of advanced classifier algorithms must be based on their
8 suitability for achieving certain objectives in specific applications (Adam et al., 2009). Because
9 mapping over large areas typically involves many satellite scenes, multi-scene mosaicking is
10 often used to group scenes into a single file set for further classification. This approach
11 optimizes both the classification process and edge matching. However, large multi-scene
12 mosaicking has essential drawback when applying to highly heterogeneous WSL wetlands. It
13 creates a variety of spectral gradients within the file (Homer and Gallant, 2001), especially
14 when the number of the appropriate scenes is limited. It results in spectral discrepancy that is
15 difficult to overcome. In this study, the advantages of consistency in class definition of the
16 scene-by-scene classification approach were considered to outweigh the inherent disadvantages
17 of edge matching and processing labor. Thus, our entire analysis was performed on a scene-by-
18 scene basis, similarly to efforts by Giri et al. (2011) and Gong et al. (2013).

19 For land cover consistency, data of the same year and season, preferably of the growing season
20 peak (July) are required. However, the main complication was the low availability of good
21 quality cloudless images of WSL during those periods. Scenes collected earlier than the 2000s
22 were very few, so they were used as substitutes for places where no other suitable imagery
23 could be found. Landsat-7 images received after 2003 were not used due to data gaps, while
24 Landsat-8 was launched after the starting our mapping procedure. Finally, we collected 70
25 suitable scenes during the peak of the growing seasons in different years. Majority of the images
26 were Landsat 5 TM scenes from July 2007. The scene selection procedure was facilitated by
27 the ability of smoothing the slight inconsistencies between images by specifying training sites
28 in overlapping areas.

29 The overall work flow involves data pre-processing, preparation of the training and test sample
30 collections, image classification on a scene-by-scene basis, regrouping of the derived classes
31 into 9 wetland complexes, the estimation of wetland ecosystem fractional coverage and

1 accuracy assessment. Atmospheric correction was not applied because this process is
2 unnecessary as long as the training data are derived from the image being classified (Song et
3 al., 2001). All of the images were re-projected onto the Albers projection. Because the WSL
4 vegetation includes various types of forests, meadows, burned areas, agricultural fields, etc.,
5 wetland environments were first separated from other landscapes to avoid misclassification. We
6 used thresholds of the Green-Red Vegetation Index (Motohka et al., 2010) to separate majority
7 of wetlands and forests. Surface water detection was performed using thresholds applied to
8 Landsat's band 5 (1.55-1.75 μm). However, because of the vegetation masking effect, detection
9 was limited to open water bodies and inundation not masked by vegetation. Thresholds were
10 empirically determined for each scene by testing various candidate values. Masked Landsat
11 images were filtered in MATLAB v.7.13 (MathWorks) to remove random noise and then
12 classified in Multispec v.3.3 (Purdue Research Foundation) using a supervised classification
13 method. The maximum likelihood algorithm was used because of its robustness and availability
14 in almost any image-processing software (Lu and Weng, 2007). All Landsat bands except the
15 thermal infrared band were used.

16 Training data plays a critical role in the supervised classification technique. Representative data
17 preparation is the most time-consuming and labour-intensive process in regional scale mapping
18 efforts (Gong et al., 2013). As a primary source of information, we used the extensive dataset
19 of botanical descriptions, photos, pH and electrical conductivity data from 28 test sites in WSL
20 (Glagolev et al., 2011). Due to vast expanse and remoteness of WSL, we still had a lack of the
21 ground truth information, which hampered training dataset construction. As a result, we had to
22 rely mostly on high-resolution images available from Google Earth. They came from several
23 satellites (QuickBird, WorldView, GeoEye, IKONOS) with different sensor characteristics;
24 multispectral images were reduced to visible bands (blue, green, red) and had spatial resolution
25 of 1-3 meters. The processing started with mapping scenes where ground truth data and high-
26 resolution images are extensively available, so the classification results could be checked for
27 quality assurance; mapping continued through adjacent images and ended at the less explored
28 scenes with poor ground truth data coverage.

29 To collect training data most efficiently, we used criteria similar to those used by (Gong et al.,
30 2013) for training sample selection: (i) the training samples must be homogeneous; mixed land-
31 cover and heterogeneous areas are avoided; and (ii) all of the samples must be at least 10 pixels
32 in size with an average sample area of approximately 100-200 pixels. The Bhattacharyya

1 distance was used as a class separability measure. The classifier was designed using training
2 samples and then evaluated by classifying input data. The percentage of misclassified samples
3 was taken as an optimistic predication of classification performance (Jain et al., 2000). When
4 accuracy of more than 80% across the training set was attained with no fields showing
5 unreasonable or unexplainable errors, the classification process was started. Classification
6 mismatch between scenes was minimized by placing training samples in overlapping areas.
7 Combining the classified images and area calculations were made using GRASS module in
8 Quantum GIS. Noise filter was applied to eliminate objects smaller than 2×2 pixels. After that,
9 a 10×10-pixel moving window was used to determine the dominant class, which was further
10 assigned to the central 4×4-pixel area.

11 **2.3 Wetland typology development**

12 As a starting point for the mapping procedure, a proper classification scheme is required.
13 Congalton et al. (2014) showed that the classification scheme alone may result in largest error
14 contribution and thus deserves highest implementation priority. Its development should rely on
15 the study purposes and the class separability of the input variables. In our case, wetland
16 mapping was initially conceived as a technique to improve the estimate of the regional CH₄
17 emissions and, secondarily, as a base to upscale other ecological functions. WSL wetlands are
18 highly heterogeneous, however, within each wetland complex we can detect relatively
19 homogeneous structural elements or “wetland ecosystems” with similar water table levels
20 (WTL), geochemical conditions, vegetation covers and, thus, rates of CH₄ emissions (Sabrekov
21 et al., 2013). To ensure a reliable upscaling, we assigned 7 wetland ecosystems in our
22 classification scheme (Fig. 1; Table 1).

23 However, wetland ecosystems generally have sizes from a few to hundreds of meters and cannot
24 be directly distinguished using Landsat imagery with 30-meter resolutions. Therefore, we
25 developed a second wetland typology that involves 9 mixed “wetland complexes” composing
26 wetland ecosystems in different proportions (Fig. 1; Table 2). The classification were adapted
27 from numerous national studies (Katz and Neishtadt, 1963; Romanova, 1985; Liss et al., 2001;
28 Lapshina, 2004; Solomeshch, 2005; Usova, 2009; Masing et al., 2010) and encompassed
29 wooded, patterned, open wetlands and water bodies. The criteria for assigning wetland
30 complexes were: (i) separability on Landsat images, and (ii) abundance in the WSL taiga zone.
31 Each wetland complex represents integral class containing several subtypes differing in
32 vegetation composition and structure. Subtypes were mapped using Landsat images and then

1 generalized into final 9 wetland complexes basing upon ecosystem similarity and spectral
2 separability.

3 To merge typologies, we estimated relative areas of wetland ecosystems within each wetland
4 complex of the final map. Depending on heterogeneity, 8 to 27 test sites of 0.1-1 km² size were
5 selected for each heterogeneous wetland complex. High-resolution images of 1-3 m resolution
6 corresponding to these areas were classified in Multispec v.3.3 using visible channels. An
7 unsupervised ISODATA classification was done on the images specifying 20 classes with a
8 convergence of 95%. Obtained classes were manually reduced to seven wetland ecosystem
9 types. Their relative proportions were calculated and then averaged among the test sites.

10 Thus, we used multiscale approach relying in two typologies. First, typology of wetland
11 complexes was used for mapping Landsat images; second, typology of wetland ecosystems was
12 used for upscaling CH₄ fluxes. The approach is similar to one devised by Peregon et al. (2005),
13 where relative area proportions of “micro-landscape” elements within SHI wetland map were
14 used for NPP data upscaling.

15 During wetland typology development, we made several assumptions. Firstly, the wetland
16 complexes were considered as individual objects, while they actually occupy a continuum with
17 no clustering into discrete units. Secondly, we assumed that all of the wetland water bodies
18 originated during wetland development have sizes less than 2×2 Landsat pixels. They are
19 represented by wetland pools and waterlogged hollows, which are structural components of
20 RHLC. The rest of the water bodies were placed into the “Lakes and rivers” class. Thirdly, in
21 this study, we only consider peatlands and water bodies; floodplain areas were separated from
22 wetlands during the classification process.

23 The concept of wetland ecosystems has merits for CH₄ emission inventory. Methane emission
24 depends mainly on water table level, temperature, and trophic state (Dise et al., 1993; Dunfield
25 et al., 1993; Conrad, 1996). We take into consideration temperature, when we upscale fluxes
26 separately for southern, middle and northern taiga. We take into consideration trophic state,
27 when we map wetland complexes using multispectral Landsat images. We take into
28 consideration water table level, when we map vegetation of wetland ecosystems with high-
29 resolution images, because vegetation reflects soil moisture conditions. We do not directly
30 consider smallest spatial elements as hummocks and tussocks. This omission introduces some
31 uncertainty in regional CH₄ emission estimate, which was evaluated by (Sabrekov et al., 2014).
32 Accordingly, reliable estimate of CH₄ fluxes accounting for fine spatial detail requires large

1 number of measurements. Such heterogeneity is being addressed by measuring fluxes in all
2 microforms in the field and then obtaining probability density distributions.

3

4 **3 Results and Discussion**

5 **3.1 Wetland map**

6 Based on Landsat imagery, we developed a high-resolution wetland inventory of the WSL taiga
7 zone (Fig. 2). The total area of wetlands and water bodies was estimated to be 52.4 Mha. West
8 Siberian taiga wetlands are noticeable even from global prospective. The global total of
9 inundated areas and peatlands was estimated to cover from 430 (Cogley, 1994) to 1170 Mha
10 (Lehner and Döll, 2004) as summarized by Melton et al. (2013); therefore, taiga wetlands in
11 WSL account for approximately from 4 to 12% of the global wetland area. Their area is larger
12 than the wetland areas of 32.4, 32, and 41 Mha in China (Niu et al., 2012), Hudson Bay Lowland
13 (Cowell, 1982) and Alaska (Whitcomb et al., 2009), respectively. The extent of West Siberia's
14 wetlands exceeds the tropical wetland area of 43.9 Mha (Page et al., 2011) emphasizing the
15 considerable ecological role of the studied region.

16 As summarized by Sheng et al. (2004), the majority of earlier Russian studies estimated the
17 extent of the entire WS's mires to be considerably lower. These studies probably inherited the
18 drawbacks of the original Russian Federation Geological Survey database, which was used as
19 the basis for the existing WSL peatland inventories (Ivanov and Novikov, 1976). This database
20 suffered from lack of field survey data in remote regions, a high generalization level and only
21 considered economically valuable peatlands with peat layers deeper than 50 cm.

22 Our peatland coverage is similar to the estimate of 51.5 Mha (Peregon et al., 2009) by SHI map
23 (Romanova et al., 1977). However, a direct comparison between the peatland maps shows that
24 the SHI map is missing important details on the wetland distribution (Fig. 3). SHI map was
25 based on aerial photography, which was not technically viable for full and continuous mapping
26 of a whole region because it is too costly and time-consuming to process (Adam et al., 2009).

27 Distribution of wetland ecosystem areas have changed significantly in comparison to SHI map
28 (Peregon et al., 2009); in particular, we obtained 105% increase in spatial extent of CH₄ high-
29 emitting ecosystems such as waterlogged, oligotrophic hollows and fens. In the case study of
30 WS's middle taiga, we found that applying the new wetland map led to a 130% increase in the

1 CH₄ flux estimate from the domain (Kleptsova et al., 2012) in comparison with the estimate
2 based on SHI map. Thus, a considerable reevaluation of the total CH₄ emissions from the whole
3 region is expected.

4 **3.2 Regularities of zonal distribution**

5 WS has a large variety of wetlands that developed under different climatic and geomorphologic
6 conditions. Concerning the wetland complex typology (excluding “Lakes and rivers” class),
7 RHCs prevail in WS’s taiga, accounting for 32.2% of the total wetland area, followed by pine
8 bogs (23%), RHLCs (16.4%), open fens (8.4%), palsa complexes (7.6%), open bogs (4.8%),
9 patterned fens (3.9%) and swamps (3.7%). Various bogs are dominant among the wetland
10 ecosystems (Table 3), while fens cover only 14.3% of the wetlands. Waterlogged hollows and
11 open water occupy 7% of the region, which is similar to the estimate by Watts et al. (2014),
12 who found that 5% of the boreal-Arctic domain was inundated during summer season.

13 The individual wetland environments have a strongly pronounced latitudinal zonality within
14 the studied region. Zonal borders stretch closely along latitude lines, subdividing the taiga
15 domain into the southern, middle, and northern taiga subzones (Fig. 2, black lines). To visualize
16 the regularities of the wetland distribution, we divided the entire area into 0.1°×0.1° grids and
17 calculated ratios of wetland ecosystem areas to the total cell areas for each grid (Fig. 4) using
18 fractional coverage data from Table 2.

19 Mire coverage of WSL’s northern taiga (62-65°N) is approximately 36%. Because of the
20 abundance of precipitation, low evaporation and slow runoff, the northern taiga is characterized
21 by largest relative area of lakes and waterlogged hollows, covering a third of the domain (Fig.
22 4a, b). Vast parts of the zone are occupied by the peatland system “Surgutskoe Polesye,” which
23 stretches for one hundred kilometers from east to west between 61.5°N and 63°N. Peatland and
24 water bodies cover up to 70% of the territory, forming several huge peatland-lake complexes
25 divided by river valleys. Northward, the slightly paludified “Sibirskie Uvaly” elevation
26 (63.5°N) divides the northern taiga into two lowland parts. Palsa hillocks appear in the
27 “Surgutskoe Polesye” region and replace the ridges and ryams to the north of the “Sibirskie
28 Uvaly” region (Fig. 4f).

29 RHCs are the most abundant in the middle taiga (59-62°N), where mires occupy 34% of the
30 area. Large wetland systems commonly cover watersheds and have a convex dome with centres
31 of 3-6 m higher than periphery. These environments have peat layer of several meters depth

1 composed of sphagnum peat with the small addition of other plants. The wetland ecosystems
2 here have distinct spatial regularities. Central plateau depressions with stagnant water are
3 covered by RHLCs. Different types of RHCs cover better-drained gentle slopes. The most
4 drained areas are dominated by ryams. Poor and rich fens develop along wetland's edges with
5 relatively high nutrient availability. Wooded swamps usually surround vast wetland systems.

6 The wetland extent reaches 28% in WS's southern taiga area (56-59°N). Wetlands are
7 composed of raised bogs alternating with huge open and patterned fens. The eastern part of the
8 subzone is dominated by small and medium-sized wetland complexes. The southern and middle
9 taiga wetlands exhibit similar spatial patterns; however, the area of fens increases southwards
10 due to the abundance of carbonate soils and higher nutrient availability. Velichko et al. (2011)
11 provide evidence for existence of a vast cold desert in the northern half of the WSL at the late
12 glacial time, whereas the southernmost part was an area of loess accumulation. The border
13 between fen and bog-dominated areas extends near 59°N and corresponds to the border between
14 the southern and middle taiga zones (Fig. 4c and e).

15 **3.3 Accuracy assessment**

16 The map accuracy assessment was based on 1082 validation polygons of 10×10 pixels that were
17 randomly spread over the WSL taiga zone. We used high-resolution images available in Google
18 Earth as the ground truth information. The confusion matrix (Table 4) was used as a way to
19 represent map accuracy (Congalton and Green, 2008). Overall, we achieved the classification
20 accuracy of 79% that can be considered reasonable for such a large and remote area. We found
21 that the accuracies for different land-cover categories varied from 62 to 99%, with the lake and
22 river, ryam, and RHC class areas mapped most successfully and open bogs and patterned fens
23 being the most confused. Some errors were associated with mixed pixels (33 polygons), whose
24 presence had been recognized by Foody (2002) as a major problem, affecting the effective use
25 of remotely sensed data in per-pixel classification.

26 Wetland complexes within large wetland systems had the highest classification accuracies. In
27 contrast, the uncertainties are particularly high for small objects. It is of special importance in
28 southern part of the domain, where highly heterogeneous agricultural landscapes neighbour
29 upon numerous individual wetlands of 100-1000 ha area. Several vegetation indices was tested
30 to map them; however, the best thresholding result was achieved by using Landsat thermal
31 band. In addition, many errors happened along the tundra boundary caused by the lack of

1 ground truth data combined with the high landscape heterogeneity. However, those small areas
2 mainly correspond to palsa complexes and have negligibly small impact on CH₄ flux estimate.
3 Misclassifications usually occurred between similar classes introducing only a minor distortion
4 in map applications. Patterned fens and open bogs were classified with the lowest producer's
5 accuracy (PA) of 62%. Patterned fens include substantial treeless areas, so they were often
6 misclassified as open fens. They were also confused with RHCs due to the similar "ridge-
7 hollow" structure. Some open bogs have tussock shrub cover with sparsely distributed pine
8 trees provoking misclassification as RHCs and pine bogs. Open fens have higher user's
9 accuracy (UA) and PA; however, visible channels of high-resolution images poorly reflect
10 trophic state, which underrates classification errors between open bogs and open fens. Swamps
11 and palsa complexes have very high PA and low UA, which is related to their incorrect
12 identification in non-wetland areas. Palsa complexes were spectrally close to open woodlands
13 with lichen layer, which covers wide areas of WSL north taiga. During dry period, swamps
14 were often confused with forests, whereas in the field they can be easily identified through the
15 presence of peat layers and a characteristic microrelief. In both cases, more accurate wetland
16 masks would lead to substantially higher accuracy levels. Lakes and rivers were classified the
17 best due to the high spectral separability of the class. They can be confused with RHLCs
18 represented by a series of small lakes or waterlogged hollows alternating with narrow
19 isthmuses. Floodplains after snow melt can also be classified as lakes (11 polygons). RHCs and
20 pine bogs were accurately identified due to their abundance in the study region and high spectral
21 separability.

22 **3.4 Challenges and future prospects**

23 The contrast between vast wetland systems and the surrounding forests is so distinct in WSL
24 that wetlands can be adequately identified by the summer season images (Sheng et al., 2004).
25 On the contrary, correct mapping of wetland with pronounced seasonal variations remains one
26 of the largest challenges. Wetlands become the most inundated after snow melt or rainy periods
27 resulting in partial transformation of oligotrophic hollows and fens into waterlogged hollows
28 (see hollows with brown Sphagnum cover at Fig. 1). Image features of swamps after drought
29 periods become similar to forests. Interannual variability of water table level in WSL wetlands
30 (Schroeder et al., 2010; Watts et al., 2014) also makes impact on mapping results.

1 New methodologies and protocols are needed to improve our ability to monitor water levels
2 (Kim et al., 2009). Observations of soil moisture and wetland dynamic using radar data such as
3 PALSAR (Chapman et al., 2015; Clewley et al., 2015) and Global Navigation Satellite Signals
4 Reflectometry are promising (Chew et al., 2016; Zuffada et al., 2015). Advanced classification
5 techniques such as fuzzy logic can be applied for mapping fine-scale heterogeneity (Adam et
6 al., 2009). Recent innovations in wetland mapping were described by Tiner et al. (2015).

7 Water table fluctuations are especially important for upscaling CH₄ fluxes because the spatial
8 distribution of methane emissions, and therefore, the total methane emission, are functions of
9 the spatial distribution of water table depths (Bohn et al., 2007). Wetland ecosystems with water
10 levels close to surface contribute most to the regional flux, while the contribution of dryer
11 ecosystems (ryams, ridges and palsa hillocks) is close to negligible (Glagolev et al., 2011;
12 Sabrekov et al., 2014).

13 Although the synergistic combination of active and passive microwave sensor data is
14 advantageous for accurately characterizing open water (Schroeder et al., 2010) and wetlands,
15 the remote sensing of water regimes is successful only when in situ data are available for
16 calibration. We still lack in situ measurements of the water table dynamics within WSL
17 wetlands. Limited monitoring have been made at the Bakchar field station (Krasnov et al., 2013;
18 Krasnov et al., 2015) and Mukhrino field station (Bleuten and Filippov, 2008); however, the
19 vast majority of obtained data are not yet analyzed and published. These measurements are of
20 special importance for the northern taiga and tundra, where shallow thermokarst lakes with
21 fluctuating water regimes cover huge areas.

22 The scarcity of reliable reference data and subsequent lack of consistency also limit the
23 accuracy of maps (Homer and Gallant, 2001). The use of ancillary data can largely improve it
24 (Congalton et al., 2014); however, more reliable classification accuracy comes with significant
25 costs regarding detailed field data. The next step in map improvement should rely on the
26 acquisition of more ground truth data for the poorly classified wetland types and remote regions.
27

28 **4 Conclusions**

29 Boreal peatlands play a major role in carbon storage, methane emissions, water cycling and
30 other global environmental processes, but better understanding of this role is constrained by the
31 inconsistent representation of peatlands on (or even complete omission from) many global land

1 cover maps (Krankina et al., 2008). In this study, we developed a map representing the state of
2 the taiga wetlands in WSL during the peak of the growing season. The efforts reported here can
3 be considered as an initial attempt at mapping boreal wetlands using Landsat imagery, with the
4 general goal of supporting the monitoring of wetland resources and upscaling the methane
5 emissions from wetlands and inland waters. The resulting quantitative definitions of wetland
6 complexes combined with a new wetland map can be used for the estimation and spatial
7 extrapolation of many ecosystem functions from site-level observations to the regional scale.
8 In the case study of WS's middle taiga, we found that applying the new wetland map led to a
9 130% increase in the CH₄ flux estimation from the domain (Kleptsova et al., 2012) comparing
10 with estimation based on previously used SHI map. Thus, a considerable reevaluation of the
11 total CH₄ emissions from the entire region is expected.

12 We estimate a map accuracy of 79% for this large and remote area. The next step in improving
13 mapping quality will depend on the acquisition of ground truth data from the least discernible
14 wetland landscapes and remote regions. Correctly distinguishing wetland complexes with
15 strongly pronounced seasonal variability in their water regimes remains one of the largest
16 challenges. This difficulty can be resolved by installing water level gauge network and usage
17 both combined remote sensing data and advanced classification techniques.

18 Our new Landsat-based map of WS's taiga wetlands can be used as a benchmark dataset for
19 validation of coarse-resolution global land cover products and for assessment of global model
20 performance in high latitudes. Although classification scheme was directed towards improving
21 CH₄ inventory, the resulting map can also be applied for upscaling of the other environmental
22 parameters.

23

24 **Acknowledgements**

25 We thank Amber Soja and anonymous reviewers for assisting in improving the initial version
26 of the manuscript. This study (research grant No 8.1.94.2015) was supported by The Tomsk
27 State University Academic D.I. Mendeleev Fund Program in 2014-2015. The study was also
28 supported by the GRENE-Arctic project by MEXT Japan.

29

30 **References**

1 Adam, E., Mutanga, O., and Rugege, D.: Multispectral and hyperspectral remote sensing for
2 identification and mapping of wetland vegetation: a review, *Wetlands Ecology and*
3 *Management*, 18, 281-296, 10.1007/s11273-009-9169-z, 2009.

4 Bleuten, W., and Filippov, I.: Hydrology of mire ecosystems in central West Siberia: the
5 Mukhrino Field Station, Transactions of UNESCO department of Yugorsky State University
6 “Dynamics of environment and global climate change”/Glagolev MV, Lapshina ED (eds.).
7 Novosibirsk: NSU, 208-224, 2008.

8 Bohn, T. J., Lettenmaier, D. P., Sathulur, K., Bowling, L. C., Podest, E., McDonald, K. C., and
9 Friborg, T.: Methane emissions from western Siberian wetlands: heterogeneity and sensitivity
10 to climate change, *Environmental Research Letters*, 2, 045015, 10.1088/1748-9326/2/4/045015,
11 2007.

12 Bohn, T. J., Melton, J. R., Ito, A., Kleinen, T., Spahni, R., Stocker, B. D., Zhang, B., Zhu, X.,
13 Schroeder, R., Glagolev, M. V., Maksyutov, S., Brovkin, V., Chen, G., Denisov, S. N., Eliseev,
14 A. V., Gallego-Sala, A., McDonald, K. C., Rawlins, M. A., Riley, W. J., Subin, Z. M., Tian, H.,
15 Zhuang, Q., and Kaplan, J. O.: WETCHIMP-WSL: intercomparison of wetland methane
16 emissions models over West Siberia, *Biogeosciences*, 12, 3321-3349, 10.5194/bg-12-3321-
17 2015, 2015.

18 Chapman, B., McDonald, K., Shimada, M., Rosenqvist, A., Schroeder, R., and Hess, L.:
19 Mapping regional inundation with spaceborne L-band SAR, *Remote Sensing*, 7, 5440-5470,
20 2015.

21 Chew, C., Shah, R., Zuffada, C., Hajj, G., Masters, D., and Mannucci, A. J.: Demonstrating soil
22 moisture remote sensing with observations from the UK TechDemoSat - 1 satellite mission,
23 *Geophysical Research Letters*, 43, 3317-3324, 2016.

1 Clewley, D., Whitcomb, J., Moghaddam, M., McDonald, K., Chapman, B., and Bunting, P.:
2 Evaluation of ALOS PALSAR data for high-resolution mapping of vegetated wetlands in
3 Alaska, *Remote Sensing*, 7, 7272-7297, 2015.

4 Cogley, J.: GGHYDRO: global hydrographic data, Peterborough, Ontario, Canada, 1994.

5 Congalton, R., Gu, J., Yadav, K., Thenkabail, P., and Ozdogan, M.: Global Land Cover
6 Mapping: A Review and Uncertainty Analysis, *Remote Sensing*, 6, 12070-12093,
7 10.3390/rs61212070, 2014.

8 Congalton, R. G., and Green, K.: Assessing the accuracy of remotely sensed data: principles
9 and practices, CRC press, Florida, USA, 2008.

10 Conrad, R.: Soil microorganisms as controllers of atmospheric trace gases (H₂, CO, CH₄, OCS,
11 N₂O, and NO), *Microbiological reviews*, 60, 609-640, 1996.

12 Cowell, D. W.: Earth Sciences of the Hudson Bay Lowland: Literature Review and Annotated
13 Bibliography, Lands Directorate, Environment Canada, 1982.

14 Dise, N. B., Gorham, E., and Verry, E. S.: Environmental factors controlling methane emissions
15 from peatlands in northern Minnesota, *Journal of Geophysical Research: Atmospheres* (1984–
16 2012), 98, 10583-10594, 1993.

17 Dunfield, P., Dumont, R., and Moore, T. R.: Methane production and consumption in temperate
18 and subarctic peat soils: response to temperature and pH, *Soil Biology and Biochemistry*, 25,
19 321-326, 1993.

20 Foody, G. M.: Status of land cover classification accuracy assessment, *Remote sensing of*
21 *environment*, 80, 185-201, 2002.

22 Frey, K. E., and Smith, L. C.: How well do we know northern land cover? Comparison of four
23 global vegetation and wetland products with a new ground-truth database for West Siberia,
24 *Global Biogeochemical Cycles*, 21, 10.1029/2006gb002706, 2007.

1 Giri, C., Ochieng, E., Tieszen, L. L., Zhu, Z., Singh, A., Loveland, T., Masek, J., and Duke, N.:
2 Status and distribution of mangrove forests of the world using earth observation satellite data,
3 *Global Ecology and Biogeography*, 20, 154-159, 10.1111/j.1466-8238.2010.00584.x, 2011.

4 Glagolev, M., Kleptsova, I., Filippov, I., Maksyutov, S., and Machida, T.: Regional methane
5 emission from West Siberia mire landscapes, *Environmental Research Letters*, 6, 045214,
6 10.1088/1748-9326/6/4/045214, 2011.

7 Gong, P., Wang, J., Yu, L., Zhao, Y., Zhao, Y., Liang, L., Niu, Z., Huang, X., Fu, H., Liu, S.,
8 Li, C., Li, X., Fu, W., Liu, C., Xu, Y., Wang, X., Cheng, Q., Hu, L., Yao, W., Zhang, H., Zhu,
9 P., Zhao, Z., Zhang, H., Zheng, Y., Ji, L., Zhang, Y., Chen, H., Yan, A., Guo, J., Yu, L., Wang,
10 L., Liu, X., Shi, T., Zhu, M., Chen, Y., Yang, G., Tang, P., Xu, B., Giri, C., Clinton, N., Zhu,
11 Z., Chen, J., and Chen, J.: Finer resolution observation and monitoring of global land cover:
12 first mapping results with Landsat TM and ETM+ data, *International Journal of Remote*
13 *Sensing*, 34, 2607-2654, 10.1080/01431161.2012.748992, 2013.

14 Gvozdetzky, N.: Physiographic zoning of USSR, MSU, Moscow, Russia, 576 pp., 1968.

15 Homer, C., and Gallant, A.: Partitioning the conterminous United States into mapping zones
16 for Landsat TM land cover mapping, Unpublished US Geologic Survey report, 2001.

17 Ivanov, K., and Novikov, S.: West Siberian peatlands, their structure and hydrological regime,
18 *Gidrometeoizdat*, Leningrad, USSR, 448 pp., 1976.

19 Jain, A. K., Duin, R. P., and Mao, J.: Statistical pattern recognition: A review, *Pattern Analysis*
20 *and Machine Intelligence*, *IEEE Transactions on*, 22, 4-37, 2000.

21 Jones, L. A., Ferguson, C. R., Kimball, J. S., Zhang, K., Chan, S. T. K., McDonald, K. C.,
22 Njoku, E. G., and Wood, E. F.: Satellite microwave remote sensing of daily land surface air
23 temperature minima and maxima from AMSR-E, *IEEE Journal of Selected Topics in Applied*
24 *Earth Observations and Remote Sensing*, 3, 111-123, 2010.

1 Katz, N., and Neishtadt, M.: Peatlands, in: West Siberia, edited by: Rihter, G. D., AS USSR,
2 Moscow, Russia, 230-248, 1963.

3 Kim, J.-W., Lu, Z., Lee, H., Shum, C. K., Swarzenski, C. M., Doyle, T. W., and Baek, S.-H.:
4 Integrated analysis of PALSAR/Radarsat-1 InSAR and ENVISAT altimeter data for mapping
5 of absolute water level changes in Louisiana wetlands, *Remote Sensing of Environment*, 113,
6 2356-2365, 10.1016/j.rse.2009.06.014, 2009.

7 Kleptsova, I., Glagolev, M., Lapshina, E., and Maksyutov, S.: Landcover classification of the
8 Great Vasyugan mire for estimation of methane emission, in: 1st International Conference on
9 “Global Warming and the Human-Nature Dimension in Siberia: Social Adaptation to the
10 Changes of the Terrestrial Ecosystem, with an Emphasis on Water Environments” (7-9 March
11 2012, Kyoto, Japan), 2012.

12 Krankina, O., Pflugmacher, D., Friedl, M., Cohen, W., Nelson, P., and Baccini, A.: Meeting the
13 challenge of mapping peatlands with remotely sensed data, *Biogeosciences*, 5, 1809-1820, 2008.

14 Krasnov, O. A., Maksutov, S. S., Glagolev, M. V., Kataev, M. Y., Inoue, G., Nadeev, A. I., and
15 Schelevoi, V. D.: Automated complex “Flux-NIES” for measurement of methane and carbon
16 dioxide fluxes, *Atmospheric and oceanic optics*, 26, 1090-1097, 2013.

17 Krasnov, O. A., Maksyutov, S. S., Davydov, D. K., Fofonov, A. V., and Glagolev, M. V. (2015).
18 Measurements of methane and carbon dioxide fluxes on the Bakchar bog in warm season. In,
19 *XXI International Symposium Atmospheric and Ocean Optics. Atmospheric Physics* (pp.
20 968066-968066-968064): International Society for Optics and Photonics

21 Kremenetski, K. V., Velichko, A. A., Borisova, O. K., MacDonald, G. M., Smith, L. C., Frey,
22 K. E., and Orlova, L. A.: Peatlands of the Western Siberian lowlands: current knowledge on
23 zonation, carbon content and Late Quaternary history, *Quaternary Science Reviews*, 22, 703-
24 723, 10.1016/s0277-3791(02)00196-8, 2003.

1 Lapshina, E.: Peatland vegetation of south-east West Siberia, TSU, Tomsk, Russia, 296 pp.,
2 2004.

3 Lehner, B., and Döll, P.: Development and validation of a global database of lakes, reservoirs
4 and wetlands, *Journal of Hydrology*, 296, 1-22, 10.1016/j.jhydrol.2004.03.028, 2004.

5 Liss, O., Abramova, L., Avetov, N., Berezina, N., Inisheva, L., Kurnishkova, T., Sluka, Z.,
6 Tolpysheva, T., and Shvedchikova, N.: Mire systems of West Siberia and its nature
7 conservation importance, Grif and Co, Tula, Russia, 584 pp., 2001.

8 Lu, D., and Weng, Q.: A survey of image classification methods and techniques for improving
9 classification performance, *International Journal of Remote Sensing*, 28, 823-870,
10 10.1080/01431160600746456, 2007.

11 Masing, V., Botch, M., and Läänelaid, A.: Mires of the former Soviet Union, *Wetlands ecology
12 and management*, 18, 397-433, 2010.

13 Matthews, E., and Fung, I.: Methane emission from natural wetlands: Global distribution, area,
14 and environmental characteristics of sources, *Global biogeochemical cycles*, 1, 61-86, 1987.

15 Melton, J. R., Wania, R., Hodson, E. L., Poulter, B., Ringeval, B., Spahni, R., Bohn, T., Avis,
16 C. A., Beerling, D. J., Chen, G., Eliseev, A. V., Denisov, S. N., Hopcroft, P. O., Lettenmaier,
17 D. P., Riley, W. J., Singarayer, J. S., Subin, Z. M., Tian, H., Zürcher, S., Brovkin, V., van
18 Bodegom, P. M., Kleinen, T., Yu, Z. C., and Kaplan, J. O.: Present state of global wetland
19 extent and wetland methane modelling: conclusions from a model inter-comparison project
20 (WETCHIMP), *Biogeosciences*, 10, 753-788, 10.5194/bg-10-753-2013, 2013.

21 Motohka, T., Nasahara, K. N., Oguma, H., and Tsuchida, S.: Applicability of green-red
22 vegetation index for remote sensing of vegetation phenology, *Remote Sensing*, 2, 2369-2387,
23 2010.

24 National Atlas of Russia, C. (2008). "Environment (Nature). Ecology": [http://xn--
25 80aaaa1bhnc1cc1cl5c4ep.xn--plai/cd2/english.html](http://xn--80aaaa1bhnc1cc1cl5c4ep.xn--plai/cd2/english.html), last access: 28 March 2016. In

1 Niu, Z., Zhang, H., Wang, X., Yao, W., Zhou, D., Zhao, K., Zhao, H., Li, N., Huang, H., Li, C.,
2 Yang, J., Liu, C., Liu, S., Wang, L., Li, Z., Yang, Z., Qiao, F., Zheng, Y., Chen, Y., Sheng, Y.,
3 Gao, X., Zhu, W., Wang, W., Wang, H., Weng, Y., Zhuang, D., Liu, J., Luo, Z., Cheng, X.,
4 Guo, Z., and Gong, P.: Mapping wetland changes in China between 1978 and 2008, *Chinese*
5 *Science Bulletin*, 57, 2813-2823, 10.1007/s11434-012-5093-3, 2012.

6 Page, S. E., Rieley, J. O., and Banks, C. J.: Global and regional importance of the tropical
7 peatland carbon pool, *Global Change Biology*, 17, 798-818, 2011.

8 Papa, F., Prigent, C., Aires, F., Jimenez, C., Rossow, W. B., and Matthews, E.: Interannual
9 variability of surface water extent at the global scale, 1993–2004, *Journal of Geophysical*
10 *Research*, 115, 10.1029/2009jd012674, 2010.

11 Peregon, A., Maksyutov, S., Kosykh, N., Mironycheva-Tokareva, N., Tamura, M., and Inoue,
12 G.: Application of the multi-scale remote sensing and GIS to mapping net primary production
13 in west Siberian wetlands, *Phyton*, 45, 543-550, 2005.

14 Peregon, A., Maksyutov, S., Kosykh, N. P., and Mironycheva - Tokareva, N. P.: Map - based
15 inventory of wetland biomass and net primary production in western Siberia, *Journal of*
16 *Geophysical Research: Biogeosciences (2005–2012)*, 113, 2008.

17 Peregon, A., Maksyutov, S., and Yamagata, Y.: An image-based inventory of the spatial
18 structure of West Siberian wetlands, *Environmental Research Letters*, 4, 045014, 2009.

19 Petrescu, A. M. R., van Beek, L. P. H., van Huissteden, J., Prigent, C., Sachs, T., Corradi, C. A.
20 R., Parmentier, F. J. W., and Dolman, A. J.: Modeling regional to global CH₄ emissions of
21 boreal and arctic wetlands, *Global Biogeochemical Cycles*, 24, 10.1029/2009gb003610, 2010.

22 Prigent, C., Papa, F., Aires, F., Rossow, W. B., and Matthews, E.: Global inundation dynamics
23 inferred from multiple satellite observations, 1993–2000, *Journal of Geophysical Research*, 112,
24 10.1029/2006jd007847, 2007.

1 Romanova, E., Bybina, R., Golitsyna, E., Ivanova, G., Usova, L., and Trushnikova, L.: Wetland
2 typology map of West Siberian lowland scale 1:2500000 GUGK, Leningrad, Russia, 1977.

3 Romanova, E.: Vegetation cover of West Siberian Lowland, in: Peatland vegetation, edited by:
4 Il'ina, I., Lapshina, E., Lavrenko, N., Meltser, L., Romanove, E., Bogoyavlenskiy, M., and
5 Mahno, V., Science, Novosibirsk, Russia, 138-160, 1985.

6 Sabrekov, A., Glagolev, M., Kleptsova, I., Machida, T., and Maksyutov, S.: Methane emission
7 from mires of the West Siberian taiga, *Eurasian Soil Science*, 46, 1182-1193, 2013.

8 Sabrekov, A. F., Runkle, B. R. K., Glagolev, M. V., Kleptsova, I. E., and Maksyutov, S. S.:
9 Seasonal variability as a source of uncertainty in the West Siberian regional CH₄ flux upscaling,
10 *Environmental Research Letters*, 9, 045008, 10.1088/1748-9326/9/4/045008, 2014.

11 Schroeder, R., Rawlins, M. A., McDonald, K. C., Podest, E., Zimmermann, R., and Kueppers,
12 M.: Satellite microwave remote sensing of North Eurasian inundation dynamics: development
13 of coarse-resolution products and comparison with high-resolution synthetic aperture radar data,
14 *Environmental Research Letters*, 5, 015003, 10.1088/1748-9326/5/1/015003, 2010.

15 Schroeder, R., McDonald, K. C., Chapman, B. D., Jensen, K., Podest, E., Tessler, Z. D., Bohn,
16 T. J., and Zimmermann, R.: Development and Evaluation of a Multi-Year Fractional Surface
17 Water Data Set Derived from Active/Passive Microwave Remote Sensing Data, *Remote
18 Sensing*, 7, 16688-16732, 2015.

19 Sheng, Y., Smith, L. C., MacDonald, G. M., Kremenetski, K. V., Frey, K. E., Velichko, A. A.,
20 Lee, M., Beilman, D. W., and Dubinin, P.: A high-resolution GIS-based inventory of the west
21 Siberian peat carbon pool, *Global Biogeochemical Cycles*, 18, 10.1029/2003gb002190, 2004.

22 Solomeshch, A.: The West Siberian Lowland, *The world's largest wetlands: ecology and
23 conservation*. Cambridge University Press, Cambridge, 11-62, 2005.

1 Solomon, S., Dahe, Q., Martin, M., Melinda, M., Kristen, A., Melinda M.B. , T., Henry, L. M.,
2 and Zhenlin, C.: Climate change 2007-the physical science basis: Working group I contribution
3 to the fourth assessment report of the IPCC, Cambridge University Press, 2007.

4 Song, C., Woodcock, C. E., Seto, K. C., Lenney, M. P., and Macomber, S. A.: Classification
5 and change detection using Landsat TM data: when and how to correct atmospheric effects?,
6 Remote sensing of Environment, 75, 230-244, 2001.

7 Tiner, R. W., Lang, M. W., and Klemas, V. V.: Remote Sensing of Wetlands: Applications and
8 Advances, CRC Press, 2015.

9 Turetsky, M. R., Kotowska, A., Bubier, J., Dise, N. B., Crill, P., Hornibrook, E. R., Minkinen,
10 K., Moore, T. R., Myers-Smith, I. H., Nykanen, H., Olefeldt, D., Rinne, J., Saarnio, S., Shurpali,
11 N., Tuittila, E. S., Waddington, J. M., White, J. R., Wickland, K. P., and Wilmking, M.: A
12 synthesis of methane emissions from 71 northern, temperate, and subtropical wetlands, Glob
13 Chang Biol, 20, 2183-2197, 10.1111/gcb.12580, 2014.

14 Usova, L.: Aerial photography classification of different West Siberian mire landscapes,
15 Nestor-History, Saint-Petersburg, 83 pp., 2009.

16 Watts, J. D., Kimball, J. S., Bartsch, A., and McDonald, K. C.: Surface water inundation in the
17 boreal-Arctic: potential impacts on regional methane emissions, Environmental Research
18 Letters, 9, 075001, 10.1088/1748-9326/9/7/075001, 2014.

19 Whitcomb, J., Moghaddam, M., McDonald, K., Kellndorfer, J., and Podest, E.: Mapping
20 vegetated wetlands of Alaska using L-band radar satellite imagery, Canadian Journal of Remote
21 Sensing, 35, 54-72, 2009.

22 Zuffada, C., Li, Z., Nghiem, S. V., Lowe, S., Shah, R., Clarizia, M. P., and Cardellach, E. (2015).
23 The rise of GNSS reflectometry for Earth remote sensing. In, *Geoscience and Remote Sensing*
24 *Symposium (IGARSS), 2015 IEEE International* (pp. 5111-5114): IEEE

25

1 Table 1. Wetland ecosystem types

Wetland ecosystem	Short description	WTL, cm (1st/2nd/3rd quartiles)¹
Open water	All water bodies greater than 2×2 Landsat pixels	-
Waterlogged hollows	Open water bodies fewer than 2×2 Landsat pixels or depressed parts of wetland complexes with WTLs above the average moss/vegetation surface	-10 / -7 / -4
Oligotrophic hollows	Depressed parts of bogs with WTLs beneath the average moss/vegetation cover	3 / 5 / 10
Ridges	Long and narrow elevated parts of wetland complexes with dwarf shrubs-sphagnum vegetation cover	20 / 32 / 45
Ryams	Extensive pine-dwarf shrubs-sphagnum areas	23 / 38 / 45
Fens	Integrated class for various types of rich fens, poor fens and wooded swamps	7 / 10 / 20
Palsa hillocks	Elevated parts of palsa complexes with permafrost below the surface	Less than 45

2 ¹ Positive WTL means that water is below average moss/soil surface; the data was taken from field dataset
3 (Glagolev et al., 2011)

4

- 1 Table 2. Wetland types and fractional coverage of wetland ecosystems (Open water – W,
- 2 Waterlogged hollows – WH, Oligotrophic hollows – OH, Ridges – R, Ryams – Ry, Fens – F,
- 3 Palsa hillocks – P)

Wetland complexes	Short description	Wetland ecosystems
<i>Wooded wetlands</i>		
Pine-dwarf shrubs-sphagnum bogs (pine bogs, ryams)	Dwarf shrubs-sphagnum communities with pine trees (local name – “ryams”) occupy the most drained parts of wetlands. Pine height and crown density are positively correlated with the slope angle. Ryams purely depend on precipitation and the atmospheric input of nutrients. The next evolutionary type under increased precipitation is RHC.	Ry: 100%
Wooded swamps	Wooded swamps develop in areas with close occurrence of groundwater. They frequently surround wetland systems; they can also be found in river valleys and terraces. Wooded swamps are extremely diverse in floristic composition and have prominent microtopography.	F: 100%
<i>Patterned wetlands</i>		
Ridge-hollow complexes (RHC)	RHC consists of alternating long narrow ridges and oligotrophic hollows. They purely depend on precipitation and the atmospheric input of nutrients. The configuration of ridges and hollows depend on the slope angle and hydrological conditions of the contiguous areas. RHCs with small, medium, and large hollows can be arranged within the class.	R: 42% OH: 58%
Ridge-hollow-lake complexes (RHLC)	RHLCs develop on poorly drained watersheds or after seasonal flooding of patterned wetlands. RHLCs are the most abundant in northern taiga. They may include numerous shallow pools. Hollows can be both oligotrophic and meso- or eutrophic.	R: 31% OH: 25% WH: 31% F: 13%
Patterned fens	Patterned fens are widely distributed within the region. They correspond to the WSL type of aapa mires. Patterned fens are composed of meso- or eutrophic hollows alternating with narrow ridges. The vegetation cover commonly includes sedge-moss communities.	R: 28% F: 72%
Palsa complexes	Palsa complexes are patterned bogs with the presence of palsa hillocks – frost heaves of 0.5-1 height. They arise in the north taiga and prevail northwards. They may include numerous shallow pools.	WH: 12% OH: 37% P: 51%
<i>Open wetlands</i>		
Open bogs	Open bogs are widespread at the periphery of wetland systems. They are characterized by presence of dwarf shrubs-sphagnum hummocks up to 30 cm in height and 50-200 cm in size.	OH: 100%
Open fens	Open fens are the integral class that encompasses all varieties of open rich and poor fens in WSL taiga. They occupy areas with higher mineral supplies at the periphery of wetland systems and along watercourses. The vegetation cover is highly productive and includes sedges, herbs, hypnum and brown mosses.	F: 100%
<i>Water bodies</i>		
Lakes and rivers	All water bodies larger than 60×60 m ² , so they can be directly distinguished by Landsat images.	W: 100%

4

5

1 Table 3. Latitudinal distribution of wetland ecosystem types

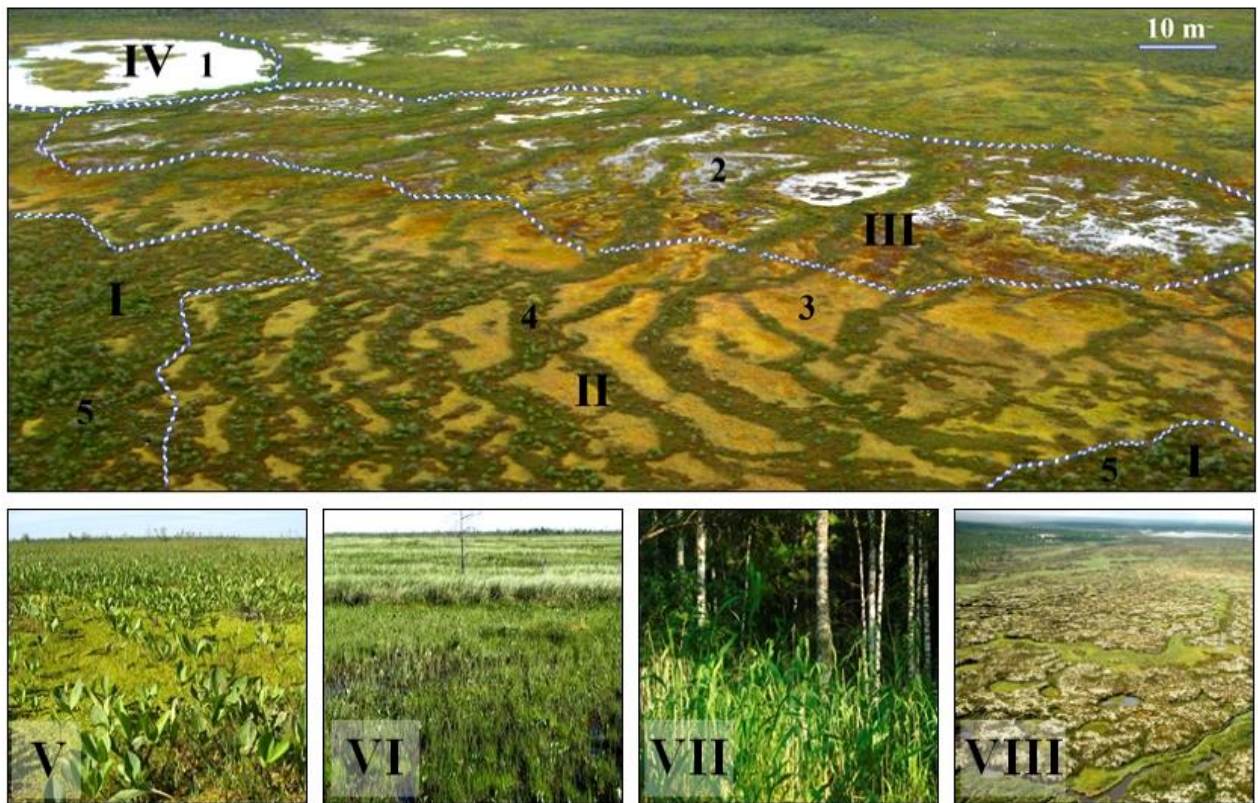
Wetland ecosystem types	South taiga		Middle taiga		North taiga		<i>Total area</i>	
	Area, Mha	%	Area, Mha	%	Area, Mha	%	Area, Mha	%
Open water	0.37	3	1.66	9	3.91	19	5.94	11.3
Waterlogged hollows	0.50	4	1.32	7	3.40	16	5.22	10.0
Oligotrophic hollows	1.87	16	5.78	30	5.60	27	13.25	25.3
Ridges	1.70	14	3.61	19	3.37	16	8.69	16.6
Ryams	3.37	28	5.14	27	1.60	8	10.11	19.3
Fens	4.22	35	1.77	9	1.53	7	7.52	14.3
Palsa hillocks	0.00	0	0.00	0	1.71	8	1.71	3.3
<i>Total wetland area</i>	<i>12.04</i>		<i>19.27</i>		<i>21.13</i>		<i>52.44</i>	
<i>Total zonal area</i>	<i>42.96</i>		<i>56.56</i>		<i>58.46</i>		<i>157.97</i>	
<i>Paludification, %</i>	<i>28.0</i>		<i>34.1</i>		<i>36.1</i>		<i>33.2</i>	

2

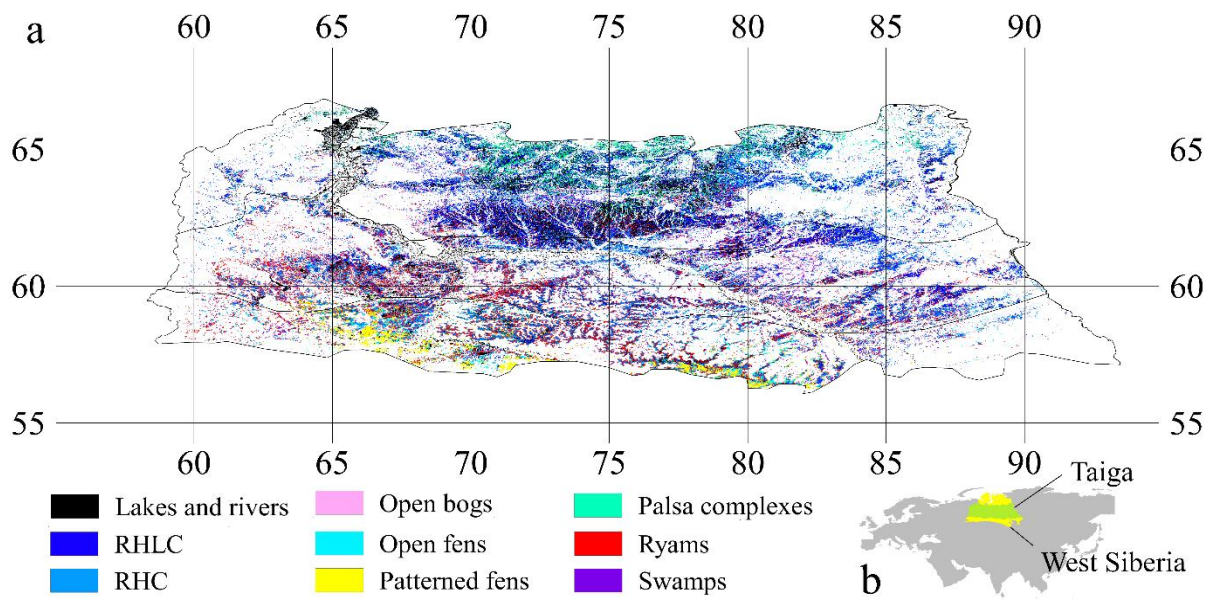
1 Table 4. Confusion matrix of West Siberian wetland map validation (additional 11 floodplain
 2 and 33 mixed class polygons classified as wetlands are not presented)

Real classes Estimated classes	Non- wetland	Lakes and rivers	RHLC	Pine bogs	RHC	Open Fens	Patterned Fens	Swamps	Palsa complexes	Open bogs	Total	UA ¹ , %
Non-wetland	110			1						2	113	97
Lakes and rivers		94	3					1			98	96
RHLC	4	7	69	1	4				2		87	79
Pine bogs	3		1	108	7		4			7	130	83
RHC	1		6	2	150	5	9			8	181	83
Open Fens			3	1	3	86	20			3	116	74
Patterned Fens	1		4	1		18	68				92	74
Swamps	5					4	9	82			100	82
Palsa complexes	13		1	2	1				54	3	74	73
Open bogs				1	7	1				38	47	81
<i>Total</i>	<i>137</i>	<i>101</i>	<i>87</i>	<i>117</i>	<i>172</i>	<i>114</i>	<i>110</i>	<i>83</i>	<i>56</i>	<i>61</i>	1038	
<i>PA², %</i>	<i>80</i>	<i>93</i>	<i>79</i>	<i>92</i>	<i>87</i>	<i>75</i>	<i>62</i>	<i>99</i>	<i>96</i>	<i>62</i>		

3

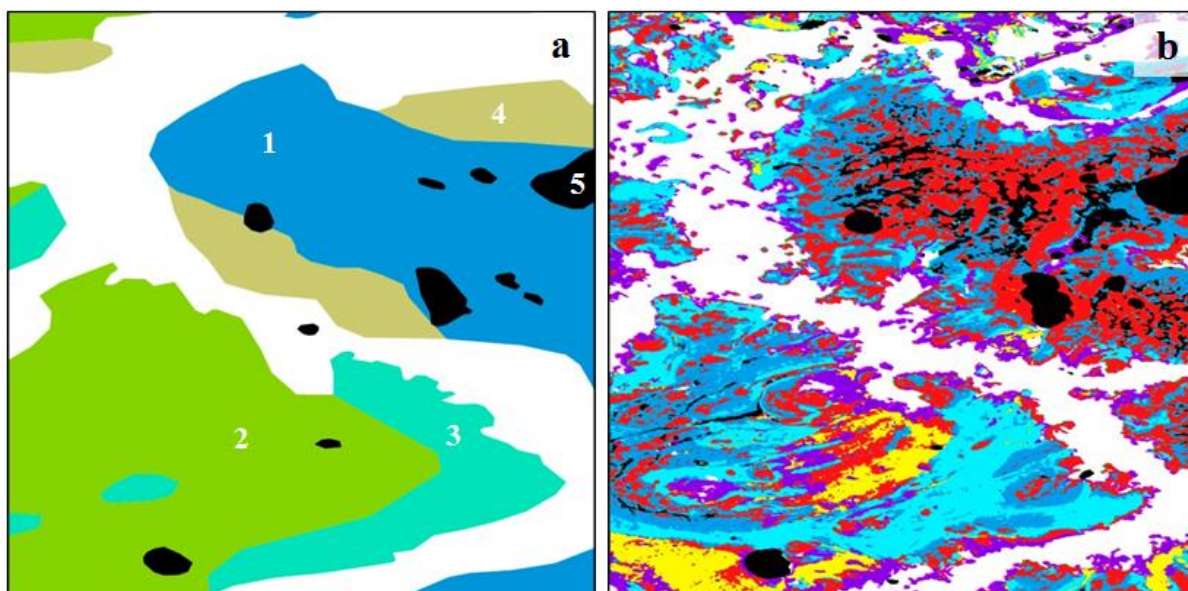


1
 2 Figure 1. Wetland complexes (I – Pine bog or ryam, II – Ridge-hollow complex or RHC, III –
 3 Ridge-hollow-lake complex or RHLC, IV – Lakes and rivers, V – Open fens, VI – Patterned
 4 fens, VII – Swamps, VIII – Palsa complexes) and ecosystems in WSL (1 – Open water, 2 –
 5 Waterlogged hollows, 3 – Oligotrophic hollows, 4 – Ridges, 5 – Ryam)

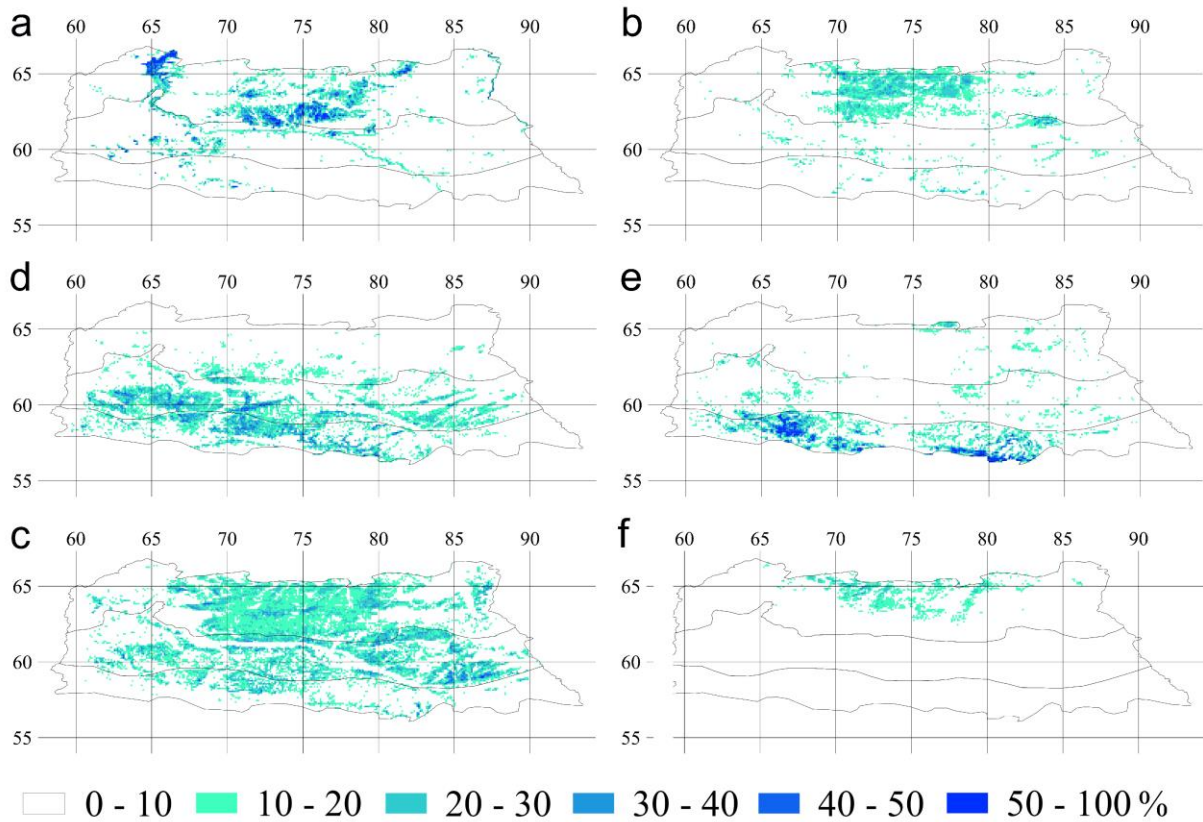


1

2 Figure 2. Wetland map (a) of the WSL taiga zone (b; yellow – WS, green – taiga zone)



1
 2 Figure 3. Comparison of wetland classifications: a – SHI map (1 – Sphagnum-dominated bogs
 3 with pools and open stand of trees, 2 – ridge-hollow, ridge-hollow-pool and ridge-pool
 4 patterned bogs, 3 – forested shrubs- and moss-dominated mires, 4 – moss-dominated treed
 5 mires, 5 – water bodies), b – this study (legend is on Figure 2); 59-59.5°N, 66-66.5°E



1

2 Figure 4. Wetland ecosystem areas for $0.1^\circ \times 0.1^\circ$ (% from the total cell area): a – open water, b
 3 – waterlogged hollows, c – oligotrophic hollows, d – ryams, e – fens, f – palsas hillocks; the
 4 distribution of ridges is not represented because it is quite similar to the oligotrophic hollow
 5 distribution; the black outlines divide the taiga into the north, middle and south taiga subzones

6